

Sensitivity of Extended X-Ray-Absorption Fine Structure to Thermal Expansion

G. Dalba, P. Fornasini, R. Grisenti, and J. Purans*

*Dipartimento di Fisica, Università degli Studi di Trento, I-38050 Povo (Trento), Italy
and Istituto Nazionale di Fisica della Materia, I-38050 Povo (Trento), Italy*

(Received 10 February 1999)

The sensitivity of extended x-ray-absorption fine structure (EXAFS) to thermal expansion has been studied by temperature-dependent measurements on germanium. The first cumulant does not reproduce the thermal expansion owing to vibrations normal to the bond. The perpendicular relative displacement $\langle \Delta u_{\perp}^2 \rangle$ has been for the first time experimentally obtained; the ratio $\langle \Delta u_{\perp}^2 \rangle / \langle \Delta u_{\parallel}^2 \rangle$ is in agreement with vibrational model calculations. Low-temperature quantum effects on the 3rd cumulant have been for the first time observed. The possibility of measuring thermal expansion from the 3rd cumulant is demonstrated, provided that quantum effects are taken into account. [S0031-9007(99)09215-7]

PACS numbers: 63.20.-e, 65.70.+y, 78.70.Dm

Extended x-ray-absorption fine structure (EXAFS) is a powerful tool for studying the local coordination and dynamics of selected atomic species in condensed matter [1]. In particular, the temperature dependence of the distance between absorber and backscatterer atoms can be used as a measure of the thermal expansion. It was early recognized that a harmonic analysis leads to an underestimation of the thermal expansion [2–4], owing to the EXAFS sensitivity to the pair potential asymmetry, while a more refined cumulant analysis [5,6] can satisfactorily take into account anharmonicity, at least for moderately disordered systems [7–10]. The EXAFS phase, which carries information on interatomic distance, is parametrized in terms of odd cumulants.

Two subtle effects have to be taken into account when a connection between first EXAFS cumulant and thermal expansion is sought: (a) Spherical nature and mean free path of the photoelectron wave; (b) thermal vibrations perpendicular to the bond direction [10–12]. The former effect leads to a difference between real and effective distributions of distances $\rho(r)$ and $P(r, \lambda) = \rho(r) \exp(-2r/\lambda)/r^2$ and their cumulants C_i^* and C_i , respectively [6], and can quite easily be accounted for. The latter effect has been for a long time neglected, in spite of its quantitative relevance; actually it represents a drawback in the determination of thermal expansion directly from EXAFS, since it has to be independently evaluated from vibrational calculations. Conversely, the difference between first EXAFS cumulant and thermal expansion could be exploited to gain original information on the correlation of vibrations normal to the bond direction.

An alternative possibility for measuring thermal expansion from EXAFS is based on the third cumulant. Classically the temperature dependence of the third cumulant is, to first order, proportional to T^2 [7,13], and thermal expansion is given by $C_3/2C_2$ [9]. Recent quantum statistical calculations have shown that quantum effects are not negligible, giving rise to a nonzero value at 0 K [14–16]; an expression connecting thermal expansion to EXAFS cumulants has been explicitly derived by Frenkel and Rehr [14].

In spite of the many theoretical papers published on these subjects in the last years [12,14–19], a comparatively minor effort has been paid to experimental studies [20,21]. In particular, to our knowledge, the very possibility of measuring thermal expansion by EXAFS with a convenient accuracy, typically better than one thousandth of an angstrom, has not yet been experimentally demonstrated. Likewise, a definite assessment of the most suitable procedure for determining thermal expansion from EXAFS data is still lacking.

In this work we present an EXAFS study of crystalline germanium in the temperature range from 10 to 600 K. The data analysis, limited to the first coordination shell and based on a phenomenological approach, has been aimed at maximizing the amount of information directly available from experimental data. An unprecedented accuracy has been achieved in the temperature dependence of the 1st and the 3rd cumulant, better than 10^{-3} Å and of the order of 10^{-5} Å³, respectively. The correlation between normal components of thermal vibrations has been for the first time measured from the first cumulant, and the result is in agreement with model calculations made for the diamond structure [22]. Quantum effects on the third cumulant have been observed, again for the first time, and taken into account in determining the anharmonic 3rd-order force constant, which in turn has allowed us to accurately reproduce the thermal expansion through the procedure suggested by Frenkel and Rehr [14]. As a result, the possibility of measuring thermal expansion from EXAFS has been demonstrated and the most suitable procedure assessed, at least for germanium.

The powdered germanium samples were prepared as in a previous experiment [23]. EXAFS at the Ge K edge was measured at the beamline DCI-D42 of LURE, Orsay, France, using a silicon (331) channel-cut monochromator. Positron energy and average current were 1.8 GeV and 200 mA, respectively. High temperature measurements (300 to 600 K) were made within a furnace, the sample being sandwiched between two graphite foils; low temperature measurements (10 to 300 K) were made within a

helium gas flow cryostat equipped with an electric heater. The temperature was stabilized to within ± 2 K. At least two spectra were recorded at each temperature. At the beginning of the analysis the edges of all spectra were aligned to within 0.1 eV.

The 1st-shell contribution, singled out by Fourier filtering within the range of photoelectron wave number 2 to 20 \AA^{-1} , was analyzed within the range 4 to 16 \AA^{-1} by the cumulant method in single scattering approximation. The analysis was based on a best fit procedure, using backscattering amplitudes, phaseshifts, and anelastic terms from the 10 K files. The relative values of the first three cumulants $\Delta C_i(T) = C_i(T) - C_i(10\text{K})$, $i = 1, 2, 3$ were treated as free parameters, while the coordination number was constrained to 4. A further refinement was carried on by analyzing every file using amplitudes, phaseshifts, and anelastic terms extracted from each of the other files, and cross comparing the results.

The statistical uncertainty of the fitting and cross-comparison procedures is represented by error bars in the figures, whenever larger than the data markers. Systematic errors of individual files can be estimated by the scattering of the cumulants values with respect to a smooth temperature dependence.

The first cumulants C_1 and C_1^* of the effective and real distributions, respectively, are connected to the distance R between the centers of thermal ellipsoids of absorber and backscatterer atoms through the equations [10]

$$C_1^* = R + \frac{\langle \Delta u_{\perp}^2 \rangle}{2R}, \quad (1)$$

$$C_1 = C_1^* - \frac{2C_2^*}{C_1^*} \left(1 + \frac{C_1^*}{\lambda} \right). \quad (2)$$

(As usual, the differences between real and effective distributions will be neglected for higher order cumulants.) The parameter λ in Eq. (2) is the photoelectron mean free path, while $\langle \Delta u_{\perp}^2 \rangle$ in Eq. (1) is the *perpendicular* component of the average relative thermal displacement of absorber and backscatterer atoms [22]:

$$\langle \Delta u^2 \rangle = \langle (\vec{u}_j - \vec{u}_0)^2 \rangle = \langle \Delta u_{\parallel}^2 \rangle + \langle \Delta u_{\perp}^2 \rangle. \quad (3)$$

The *radial* component $\langle \Delta u_{\parallel}^2 \rangle$, or mean square relative displacement (MSRD) [24], corresponds to a good approximation to the 2nd cumulant:

$$\langle \Delta u_{\parallel}^2 \rangle = \langle [\hat{R} \cdot (\vec{u}_j - \vec{u}_0)]^2 \rangle \approx C_2^* \approx C_2. \quad (4)$$

Equation (2) can be inverted to get a workable relation between cumulants of the effective and real distributions by substituting C_1^* in the last term with a constant approximate crystallographic distance $R' = 2.45 \text{ \AA}$:

$$\Delta C_1^* \approx \Delta C_1 + \frac{2\Delta C_2}{R'} \left(1 + \frac{R'}{\lambda} \right). \quad (5)$$

In Fig. 1a the relative values ΔC_1^* obtained from Eq. (5) for $\lambda = 6$ and 12 \AA (upper and lower circles, respectively) are compared with the experimental relative values ΔC_1 (squares). The continuous line in Fig. 1a represents the thermal expansion ΔR calculated from the linear expansion curves 4 and 9 of Ref. [25]. As expected from Eq. (5), ΔC_1^* grows with temperature faster than ΔC_1 . Moreover, both ΔC_1^* and ΔC_1 grow faster than ΔR ; a similar behavior was found for AgI and CdSe [10,11].

The difference between ΔC_1^* and ΔR is due to the growth with temperature of the perpendicular relative displacement term $C_{\perp} = \langle \Delta u_{\perp}^2 \rangle$. Equation (1) can be easily inverted to give the values ΔC_{\perp} relative to the low temperature spectrum: $\Delta C_{\perp} = 2R'(\Delta C_1^* - \Delta R)$.

Absolute values of the MSRD $C_2 = \langle \Delta u_{\parallel}^2 \rangle$ were obtained by fitting an Einstein model to the experimental relative values ΔC_2 ; the best fitting Einstein frequency was $\nu_{\parallel} = 7.55 \text{ THz}$. An analogous procedure was devised for calculating the absolute values $C_{\perp} = \langle \Delta u_{\perp}^2 \rangle$ from the

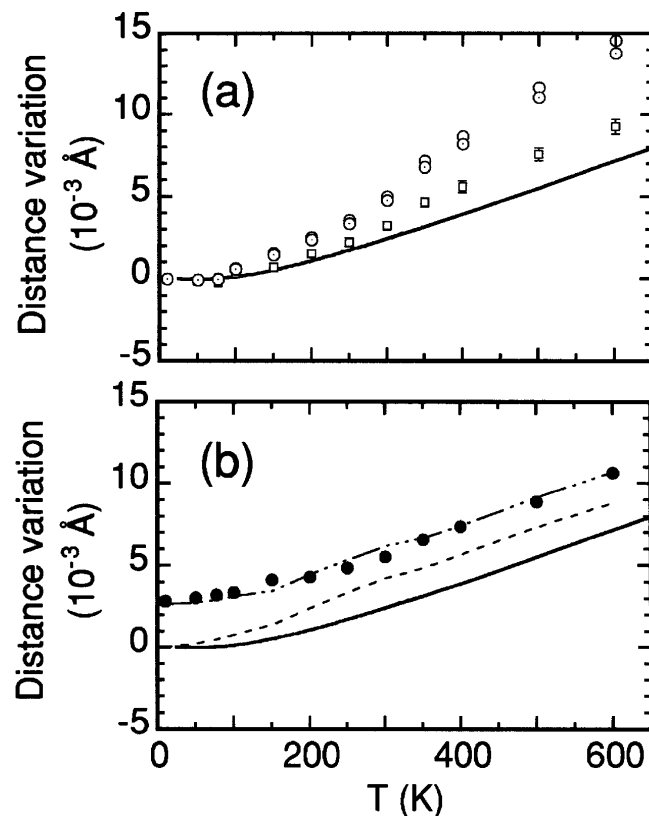


FIG. 1. Comparison between the 1st-shell thermal expansion of germanium from Ref. [25] (full line in both panels) and different parameters from EXAFS: (a) relative first cumulants ΔC_1 (squares with error bars) and ΔC_1^* (circles) of effective and real distributions, respectively; upper and lower circles are from Eq. (5) with $\lambda = 6$ or 12 \AA , respectively. (b) $\Delta C_3/2C_2$, classical approximation for the 3rd cumulant (dashed line), $C_3/2C_2$, quantum treatment of the 3rd cumulant (dash-dotted line), and net thermal expansion a according to Ref. [14] (full circles).

relative ones ΔC_{\perp} . The result of the Einstein fit was not unique, depending on the choice of the mean free path λ in Eq. (5) and the temperature range considered; a shorter range 10–300 K is more reliable than the entire range 10–600 K, in view of the highest signal-to-noise experimental ratio and the weaker influence of anharmonicity in transverse vibrations. The Einstein frequency ν_{\perp} varied from 2.9 to 3.2 THz for the different conditions, being higher for the higher λ value and the shorter fitting range. The absolute values of C_2 and C_{\perp} are shown in Fig. 2a.

Like the MSRD $C_2 = \langle \Delta u_{\parallel}^2 \rangle$, also the perpendicular component $C_{\perp} = \langle \Delta u_{\perp}^2 \rangle$ carries peculiar information on the correlation of atomic thermal motion; its values experimentally obtained from EXAFS are an independent test of eigenfrequencies and eigenvectors from vibrational models or *ab initio* calculations. On the ground of symmetry considerations, one can show that the ratio between

the two components, in a lattice with the diamond structure [22], is

$$\gamma = \frac{\langle \Delta u_{\perp}^2 \rangle}{\langle \Delta u_{\parallel}^2 \rangle} = 2 + 12 \frac{\langle u_x(0) u_y(1) \rangle}{\langle \Delta u_{\parallel}^2 \rangle}. \quad (6)$$

The cross-correlation term $\langle u_x(0) u_y(1) \rangle$ depends on the peculiar vibrational properties of the crystal. The ratio γ experimentally determined for germanium in this work is compared in Fig. 2b with the same ratio calculated for silicon using an adiabatic bond charge model [22]. The overall agreement is good; the residual discrepancy can be attributed to silicon having a Debye temperature 1.8 times higher than germanium, as can be seen by calculating the ratio γ for silicon with frequencies ν_{\parallel} and ν_{\perp} 1.8 times higher than those for germanium (dotted and dash-dotted lines in Fig. 2b).

The third cumulant C_3 , in first-order classical approximation, has a parabolic dependence on temperature [7]. Actually, in systems with relatively low Debye temperatures, like AgI and CdSe, the experimental values ΔC_3 were consistent with a T^2 behavior; as a consequence, low temperature quantum effects were considered negligible and the absolute value of C_3 could be assumed equal to zero at 0 K, so that $C_3 = \Delta C_3$ [10,11]. In the present case of germanium, on the contrary, the experimental ΔC_3 values are characterized by a flat region at low temperatures (Fig. 3), which can reasonably be attributed to a deviation from the classical T^2 approximation.

Expressions for the net thermal expansion and the second and third cumulants as a function of the 2nd- and 3rd-order force constants of the effective potential have been derived by Frenkel and Rehr [14] using a perturbative quantum approach in quasiharmonic approximation.

The 2nd order force constant $k = 8.5 \text{ eV}/\text{\AA}^2$ was directly obtained from the Einstein frequency of the

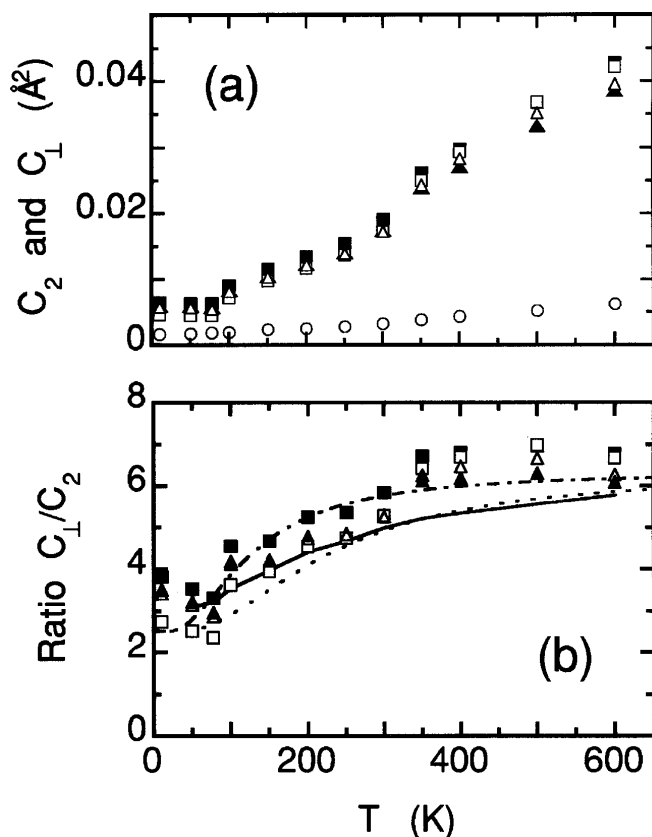


FIG. 2. (a) Absolute values of C_2 (open circles, larger than the error bars) and C_{\perp} (squares and triangles refer to $\lambda = 6$ and 12, respectively; full and open symbols refer to Einstein fits extended to 600 K or limited to 300 K, respectively.) (b) Ratio $\gamma = C_{\perp}/C_2$ for germanium determined from EXAFS: squares and triangles as in panel (a); the dash-dotted line is the ratio between the Einstein models with frequencies $\nu_{\perp} = 3$ THz and $\nu_{\parallel} = 7.55$ THz. The continuous line is the ratio calculated for silicon through an adiabatic bond charge model [22]; the dashed line is the ratio between the Einstein models with frequencies scaled by a factor 1.8 with respect to the frequencies of germanium.

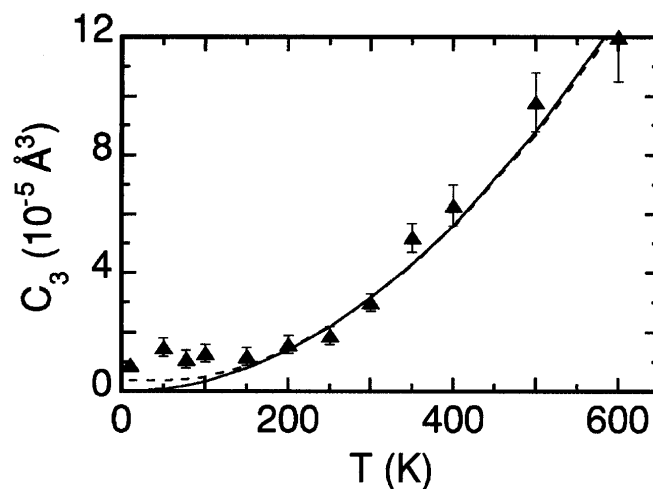


FIG. 3. Absolute values of the 3rd cumulant (triangles) obtained by fitting a T^2 parabola (continuous line) to the experimental relative values ΔC_3 above 200 K. The dashed line is the corresponding model of Frenkel and Rehr [14].

MSRD. The variation of k with thermal expansion expected in quasiharmonic approximation was estimated of the order of 3 percent, and neglected. The 3rd order force constant $k_3 = -4.8 \text{ eV}/\text{\AA}^3$ was obtained by fitting a parabola (continuous line in Fig. 3) to the experimental ΔC_3 values for $T > 200 \text{ K}$, where quantum effects are negligible. No significative variations in k_3 were anyway found by lowering the minimum of the fitting range to 150 or 100 K. A nonzero absolute value of C_3 of the order of $1 \times 10^{-5} \text{ \AA}^3$ was in this way obtained at 0 K (triangles in Fig. 3). The absolute values of C_3 calculated through Eq. (18) of Ref. [14] are shown in Fig. 3 as a dashed line.

We can now evaluate the information on thermal expansion attainable from the 3rd cumulant (Fig. 1b). If classical approximation is assumed ($C_3 = \Delta C_3 = 0$ at 0 K), the values $\Delta C_3/2C_2$ (dashed line) overestimate thermal expansion. On the contrary, the net thermal expansion $a = -3k_3 C_2/k$ as defined by Frenkel and Rehr [14] has the same temperature dependence (full circles) as the values from Ref. [25]; the difference in absolute values of about $3 \times 10^{-3} \text{ \AA}$ is due to the shift of the equilibrium position at 0 K with respect to the minimum of the effective potential. If quantum effects are taken into account in the determination of C_3 (dashed line in Fig. 3), the ratio $C_3/2C_2$ (dash-dotted line in Fig. 1b) is equivalent to the net thermal expansion a , in spite of the difference of analytical expressions.

The experimental determination of thermal expansion of germanium from EXAFS cannot be based on the first cumulant, but is possible from the third cumulant, provided that low temperature quantum effects are properly taken into account. This means that the spherical nature of photoelectron wave and the thermal vibrations normal to the bond direction affect the first but not the third cumulant, or, otherwise stated, the position but not the shape of the effective pair potential.

In conclusion, this work demonstrates the possibility of obtaining information on the correlation of vibrations normal to the bond direction from EXAFS spectra. This kind of information is not easily available from other experimental techniques. The simple procedure here proposed is applicable to both crystalline and amorphous materials.

As far as thermal expansion is concerned, a generalization of the present results is far from trivial. As a matter of fact, in AgI and CdSe the ratio $C_3/2C_2$ is much larger than thermal expansion, while a downward shift of the potential minimum is noticed [10,11]. A broader and deeper understanding of the effects of thermal expansion on EXAFS of crystals would open new perspectives for the study of local thermodynamical properties in nanocrystalline materials as well as in multicomponent glasses.

The authors are indebted to F. Rocca for sample preparation, A. Traverse and F. Villain for assistance in measurements, and F. Monti and D. Pasqualini for helpful discussions.

*Permanent address: Institut of Solid State Physics, University of Latvia, LV-1603 Riga, Latvia.

- [1] *X-ray Absorption*, edited by D.C. Koningsberger and R. Prins (Wiley, New York, 1988).
- [2] P. Eisenberger and G.S. Brown, *Solid State Commun.* **29**, 481 (1978).
- [3] T.M. Hayes, J.B. Boyce, and J.L. Beeby, *J. Phys. C* **11**, 2931 (1978).
- [4] E.D. Crozier and A. Seary, *Can. J. Phys.* **58**, 1388 (1980).
- [5] G. Bunker, *Nucl. Instrum. Methods Phys. Res.* **207**, 437 (1983).
- [6] E.D. Crozier, J.J. Rehr, and R. Ingalls, in *X-ray Absorption*, edited by D.C. Koningsberger and R. Prins (Wiley, New York, 1988).
- [7] J.M. Tranquada and R. Ingalls, *Phys. Rev. B* **28**, 3520 (1983).
- [8] E.A. Stern, Y. Ma, O. Hanske-Petitpierre, and C. Bouldin, *Phys. Rev. B* **46**, 687 (1992).
- [9] L. Tröger, T. Yokoyama, D. Arvanitis, T. Lederer, M. Tischer, and K. Baberschke, *Phys. Rev. B* **49**, 888 (1994).
- [10] G. Dalba, P. Fornasini, R. Grisenti, D. Pasqualini, D. Diop, and F. Monti, *Phys. Rev. B* **58**, 4793 (1998).
- [11] G. Dalba, P. Fornasini, R. Gotter, and F. Rocca, *Phys. Rev. B* **52**, 149 (1995).
- [12] E.A. Stern, *J. Phys. IV (France)* **7**, C2, 137 (1997).
- [13] E.A. Stern, P. Livins, and Z. Zhang, *Phys. Rev. B* **43**, 8850 (1991).
- [14] A.I. Frenkel and J.J. Rehr, *Phys. Rev. B* **48**, 585 (1993).
- [15] T. Fujikawa and T. Miyanaga, *J. Phys. Soc. Jpn.* **62**, 4108 (1993).
- [16] T. Miyanaga and T. Fujikawa, *J. Phys. Soc. Jpn.* **63**, 1036 (1994).
- [17] T. Ishii, *J. Phys. Condens. Matter* **4**, 8029 (1992).
- [18] N. Van Hung and J.J. Rehr, *Phys. Rev. B* **56**, 43 (1997).
- [19] A.B. Edwards, D.J. Tildesley, and N. Binsted, *Mol. Phys.* **91**, 357 (1997).
- [20] O. Kamishima, T. Ishii, H. Maeda, and S. Kashino, *Solid State. Commun.* **103**, 141 (1997).
- [21] T. Yokoyama, T. Ohta, and H. Sato, *Phys. Rev. B* **55**, 11 320 (1997).
- [22] O.H. Nielsen and W. Weber, *J. Phys. C* **13**, 2449 (1980).
- [23] G. Dalba, P. Fornasini, M. Grazioli, and F. Rocca, *Phys. Rev. B* **52**, 11 034 (1995).
- [24] G. Beni and P.M. Platzman, *Phys. Rev. B* **14**, 1514 (1976).
- [25] Y.S. Touloukian, R.K. Kirby, R.E. Taylor, and P.D. Desai, *Thermophysical Properties of Matter* (Plenum, New York, 1977), Vol. 13.